EXPERIMENTAL AND NUMERICAL INVESTIGATION OF THE HYGROTHERMAL BEHAVIOUR OF CORK CONCRETE PANELS IN NORTH ALGERIA

Chadi Maalouf[a], Hocine Boussetoua[a,b], Tala Moussa[a], Mohammed Lachi[a], Azzedine Belhamri[c]
[a]GRESPI EA 4694 University of Reims Champagne-Ardenne Reims, France
[b]Laboratory of Applied Energetics and Materials, University of Jijel, Faculty of Technology, Jijel, Algeria.
[c]Laboratory for Climate Engineering, University of Constantine 1, Faculty of Technology, Constantine, Algeria.

ABSTRACT

The paper presents a laboratory investigation about cork-cement mixtures designed for building applications. Samples are prepared by mixing cork aggregates, sand, cement and water. Two volume dosages of cork are considered by 50% and 75% (relative to sand). The samples are then characterized in terms of their hygrothermal properties, which are used for simulations on room level for the Constantine city in Algeria. Results show that using cork concrete results in the energy consumption economy that can reach 29% when compared to a classical solution using hollow brick.

INTRODUCTION

The use of local materials is one of the interesting solutions that can reduce energy consumption and leads to better environmental protection. Among the new materials subject of current research, incorporating vegetal aggregate materials such as cork into a cement matrix seems to be an interesting solution due to the thermal conductivity reduction. Cork is a natural product that has important features that make it both useful and necessary for several branches of industrial activity, particularly in the building construction.

The natural habitat of the cork oak is the perimeter of the western Mediterranean basin (present for over 60 million years). Cork is a low density material and provides excellent thermal and acoustic insulation (Aziz *et al*. 1979, Moreira *et al*. 2014). It is a renewable resource, whose harvest preserves the trees and helps to improve their health and prolong their lives.

The combination of cork aggregates and a cementitious binder creates a building material with mechanical and hygrothermal properties that differ from those of conventional concrete. According to Moreira et al., compressive strengths for such materials ranged from 0.2 MPa to 2.23 MPa and their thermal conductivity varied from 0.194 to 0.318 W/m K depending on their cork content.

In this paper, the authors present preliminary results of the development of a new material made of cement and cork aggregates, its physical properties and application to build in the Constantine area in Algeria.

First, material is presented and its hygrothermal properties are measured and shown. These properties are then used in simulation in order to assess material hygrothermal performance. Simulations are run for a period of one year on room level and the results are compared to those obtained with the classical construction techniques used in the region.

MATERIALS

The materials used in the preparation of our samples are : crushed sand, cork granules obtained after grinding pieces of natural cork to size lesser than 6.3 mm, Portland cement (CEM II / BL 32.5 N) and water. Two mixtures were prepared by replacing a proportion of sand with another of cork granules with 50 and 75% of cork granules in volume (respectively noted L50 and L75). The cement content depends on sand amount (1/3 in mass) and water on cement content (1/2 in mass).

Details of mixes composition and their mass density at dry state are given in Table 1. For each mixture, samples are produced by mixing sand, cork and cement in a mixer then water is added gradually until a homogeneous mixture is obtained. The latter mixture is moulded and slightly compacted in wooden moulds, then left to stabilize at room conditions (21°C, 50% RH).

Sample	Sand (Kg / m^3)	Cork granules (Kg / m^3)	Cement (Kg / m^3)	Water (Kg / m^3)	Mass density (Kg / m^3)
L50	557.9	36.8	186	93	1590
L75	323.3	64	107.8	54	900

Table 1: Mixes composition for the studied cement-cork materials and their mass density at dry state.

HYGROTHERMAL PROPERTIES

Moisture buffer value

The Moisture Buffering Value (MBV) is defined as the amount of moisture absorbed or released from the material per unit area when it is exposed to a daily periodic variation of relative humidity under isothermal conditions. It is expressed in g / (m² % RH) and determined according to the Nordtest protocol (Rode, 2005). The MBV value is a direct measure of the amount of moisture transported to and from a material when the exposure is given. Physically, the MBV can be associated with the effusivity for moisture exchange, a definition parallel to thermal effusivity (Hagentoft, 2001).

For this test, the edges and the backsides of samples are sealed in order to obtain one-dimensional moisture flow. For each formulation, four samples of 10x10x5 cm^3 are used. They are stabilised to 23 ± 0.5 °C and 50 ± 2% RH in a climatic chamber binder MKF 720 and weighed until the equilibrium is reached. After stabilization, the protocol defines a cyclic step-changes in relative humidity between high (75%) and low (33%) values for 8 hours and 16 hours respectively, until the change in mass is less than 5% between the last three cycles (Rode, 2005). The asymmetry in time scheme is twofold: (1) It replicates the daily cycle seen in many rooms, e.g. offices or bedrooms, where the load comes in approximately 8 hours, and (2) for practical reasons during testing if the climatic chamber conditions are changed manually, it is a scheme, which is easier to keep than a 12 h + 12 h shift (Rode, 2005).

The step changes in relative humidity are achieved within 10 min from low to high RH and within 30 min from high to low RH. The change in mass Δm of the sample during the uptake period gives the practical MBV in g/(m^2%RH). Samples are weighted during adsorption and desorption period, five measurements at high relative humidity and two measurements at low relative humidity. The practical MBV is calculated by:

$$MBV_{practical} = \frac{\Delta m}{A * (RH_{high} - RH_{low})} \quad (1)$$

Where A is the area of the specimen, RH_{high} is the highest relative humidity and RH_{low} is the lowest.

Figure 1: The samples manufactured for MBV measuring.

Figure 1 shows the L75 samples used for the MBV measurement and Figure 2 shows the variation of the mass of a sample of 75% of cork during the MBV test.

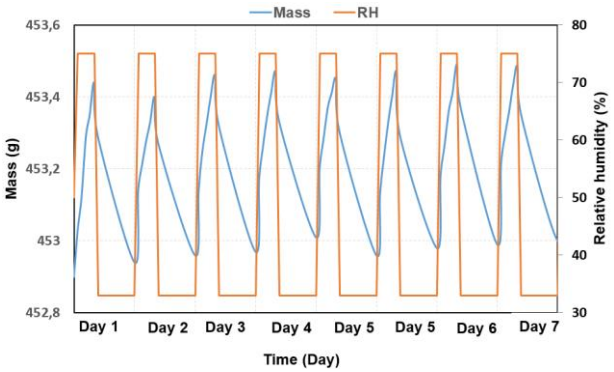

Figure 2: Change in mass as a function of time, at a relative humidity between 75% -33% for a sample of L75.

The results give an average MBV value of 1.2 g m^{-2} $\%HR^{-1}$ for the L75 composition and 0.42 g m^{-2} $\%HR^{-1}$ for the L50 composition. These results show that the L75 composition has a good moisture buffering capacity and can be classified as a good humidity regulator since its moisture buffering value (1.2) is between 1 and 2.

By comparing this value with other materials used in civil engineering (Rode, 2005), we find that this value is much higher than plasters but remains lower than that of hemp-lime or hemp starch composites. This difference in behavior is mainly due to the nature of the binder used which in our case is the cement, that it is less hydrophilic than lime or starch.

Sorption curve

The adsorption isotherm was determined according to the European standard EN NF ISO 12571 ((NF EN ISO, 2001) using the desiccators method.

There were tested four samples of each composition of 10×10×3 cm^3. The hygroscopic salts used were $MgCl_2$, $Mg(NO_3)_2$, NaCl, KCl and KNO_3 giving

relative humidities of 33%, 53% , 75%, 84% and 94% respectively. The desiccators were placed in a climatic chamber at 23 °C and 50 % relative humidity.

The moisture content by mass u (Kg/Kg) was calculated according to the equation:

$$u = \frac{m - m_0}{m_0} = \frac{m_w}{m_0} \quad (2)$$

where m (Kg) is the mass of wet specimen, m_0 (Kg) mass of the dry specimen at 0% relative humidity, m_w is the mass of water content. Initially specimen are dried in an oven at 50°C till mass stabilization.

The adsorption isotherms of cork concrete were determined for L75 and L50 and curves are shown in Figure 3. Each point on the curve is the average of four experimental values.

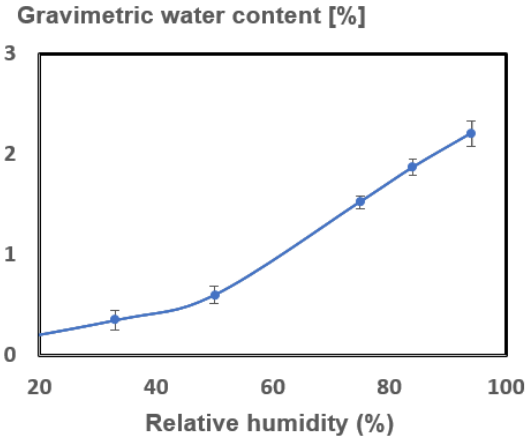

(a)

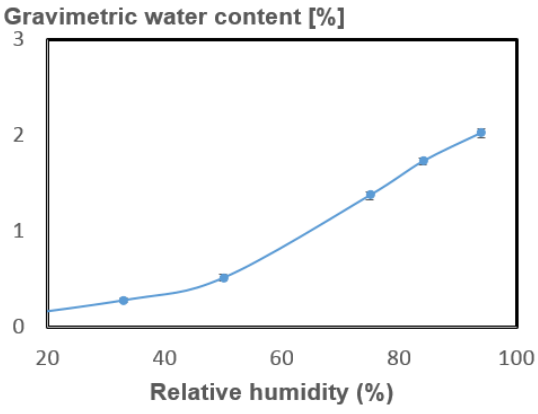

(b)

Figure 3: Adsorption curve for L75 (a) and L50 (b).

The relationship between water content and the relative humidity of the air is a non-linear increasing function. The adsorption isotherms show that when the relative humidity increases the moisture content of the samples tested and therefore increases the curve increases.

The results show that (L75) has a higher water content than the cork concrete (L50), since it has a greater porosity. In both cases, the sorption isotherm has the same shape and belongs to the type 2 in the classification of IUPAC (IUPAC, 1985). It is adjusted with the least square method using the following analytical expression (Merakeb, 2008) where a, b and u_{sat} are given in the Table 2:

$$ln\left(\frac{u}{u_{sat}}\right) = a\ln(\varphi)\ln(b * \varphi) \quad (3)$$

	u_{sat}	a	b
L75	3.213	1.39	1.018
L50	2.723	1.77	0.503

Table 1 : Values of the coefficients of the sorption curve for the L75 and L50 specimen, as determined using the least square method.

Water vapour permeability

Water vapor permeability tests are carried out with the cup method according to NF EN ISO standard 12571 (NF EN ISO, 2000).

The cup method consists in sealing a vapor tight cup containing a desiccant or saturated salt solution, with the test material. Before measurements, samples were dried and stored at 50% relative humidity and 23°C until the stabilization of their weight. After that, specimens are insulated on all lateral sides with a waterproof adhesive, put into the cup, and sealed with a gasket. The desiccant or saturated salt solution will ensure a constant relative humidity below the sample at constant temperature.

The dry cup test is conducted with the given relative humidities of 0 % and 50 %. The vapour flux goes from higher relative humidity to lower relative humidity through the sample of thickness d (m). Regular gravimetric measurements of the cup are used to determine the weight gain (or loss) of the cup and hence the moisture flux g ($kg.m^{-2}\ s^{-1}$) through the specimen.

Water vapor permeability δ presented in equation (4) is determined by applying Fick's law at steady state.

$$\delta = \frac{g * d}{\nabla p_v} \quad (4)$$

$$\mu = \frac{\delta_a}{\delta} \quad (5)$$

Where μ is the material vapour diffusion resistance factor and δ_a ($Kg.m^{-1}.s^{-1}.Pa^{-1}$) is the air vapour permeability. Actually, only dry cup test results are available and are shown in Table 3.

Sample	μ value (dry cup)
L75	10
L50	60

Table 2 : Dry cup test results for the L75 and L50 specimens.

Thermal conductivity

In order to have data on the heat transfer in these materials, their thermal conductivity was measured at dry state and at 50 % RH with the flow meter method and according to the international standard EN 12667 (EN 12667, 2001). These measurements are performed on samples of dimensions 20x20x3 cm^3. Three samples of each composition are used as shown in Figure 4.

Figure 4: L75 Samples used for the measurement of thermal conductivity.

Measurements of thermal conductivity obtained were performed at a temperature difference of 8°C between the two faces. The average temperature of the sample is 23°C. The measurement results are given in Table 4.

Sample	Dry state	At 50%
L75	0.194	0.25
L50	0.349	0.45

Table 4: Thermal conductivities at dry state and 50% relative humidity (W m^{-1} K^{-1}).

From these results one can deduce that the L75 has the lowest thermal conductivity at the dry state of 0.194 W m^{-1} K^{-1} This low value is primarily due to the high percentage of cork granules (75% compared to cork sand volume).

Gradually, as the proportion of cork increases, the thermal conductivity decreases. When relative humidity increases, thermal conductivity increases as material moisture content increases.

NUMERICAL STUDY

Mathematical models

Mechanisms of moisture transport in a single building material have been extensively studied by ((Künzel, 1995), (Perdesen, 1992), (Mendes *et al*., 1997)). Most of the models have nearly the same origin Philip and the de Vries model (Philip *et al.*, 1957). In this article, Umidus model (Mendes *et al*., 1997) is used, in which moisture is transported under liquid and vapour phases. The mass conservation equation is then:

$$\frac{\partial \theta}{\partial \tau} = \frac{\partial}{\partial x}\left(D_T \frac{\partial T}{\partial x}\right) + \frac{\partial}{\partial x}\left(D_\theta \frac{\partial \theta}{\partial x}\right) \quad (6)$$

With the boundary conditions (x = 0 and x = L)

$$-\rho_l \left(D_T \frac{\partial T}{\partial X} + D_\theta \frac{\partial \theta}{\partial x}\right)\Big|_{x=0,e} = h_{M,e}\left(\rho_{v,a,e} - \rho_{v,s,e}\right) \quad (7)$$

$$-\rho_l \left(D_T \frac{\partial T}{\partial X} + D_\theta \frac{\partial \theta}{\partial x}\right)\Big|_{x=L,i} = h_{M,i}\left(\rho_{v,s,i} - \rho_{v,a,i}\right) \quad (8)$$

with $D_T = D_{Tl} + D_{Tv}$ and $D_\theta = D_{\theta l} + D_{\theta v}$, where D_{Tl} is the liquid phase transport coefficient associated to a temperature gradient, D_{Tv}, vapor phase transport coefficient associated to a temperature gradient, $D_{\theta l}$, liquid phase transport coefficient associated to a moisture content gradient, $D_{\theta v}$, vapor phase transport coefficient associated to a moisture content gradient, D_T, mass transport coefficient associated to a temperature gradient and D_θ, mass transport coefficient associated to a moisture gradient.

$$D_\theta = \frac{\delta_a}{\mu}\frac{P_{vs}}{\rho_0}\frac{1}{\xi} \quad (9)$$

Vapour transport coefficient under a temperature gradient is given by the relation:

$$D_{T,ve} = \phi \frac{\delta_a}{\rho_l \mu}\frac{dP_{vs}}{dT} \quad (10)$$

One dimensional model of the energy conservation equation with coupled temperature and moisture for a porous media is considered, and the effect of the

absorption or desorption heat is added. This equation is written as:

$$\rho\, Cp_m \frac{\partial T}{\partial \tau} = \frac{\partial}{\partial x}\left(\lambda(T,\theta)\frac{\partial T}{\partial x}\right) + L_v \rho_l \left(\frac{\partial}{\partial x}\left(D_{T,v}\frac{\partial T}{\partial x}\right) + \frac{\partial}{\partial x}\left(D_{\theta,v}\frac{\partial \theta}{\partial x}\right)\right) \quad (11)$$

$$Cp_m = Cp_{0+} Cp_l \frac{\rho_l}{\rho_\theta} \quad (12)$$

Where Cp_m is the average specific capacity, which takes into account the dry material specific heat and the contribution of the specific heat of the liquid phase. λ is the thermal conductivity depending on moisture content.

Boundary conditions take into account radiation, heat and phase change.

$$-\lambda\frac{\partial T}{\partial x}\Big)_{x=0,e} - L_v\,\rho_l\,\left(D_{T,v}\frac{\partial T}{\partial x} + D_{\theta,v}\frac{\partial T}{\partial x}\right)_{x=0,e} = h_{T,e}\,\left(T_{a,e} - T_{s,e}\right) + L_v\,h_{M,e}\,\left(\rho_{ve,a,e} - \rho_{ve,s,e}\right) + \Phi_{ray,e} \quad (13)$$

Air model

The net heat transferred into the room across its faces must equal the heat stored in the volume of air in the room. That involves heat fluxes through the envelope (transmission, long and short-wave radiation input), additional thermal loads, air exchange due to natural convection or HVAC and thermal losses due to thermal heat bridges. The energy equation can be written as:

$$\left(\rho_i C_p V + I\right)\frac{\partial T}{\partial \tau} = \emptyset_{West} - \emptyset_{East} + \emptyset_{South} - \emptyset_{North} + \emptyset_{Bottom} - \emptyset_{Top} + \emptyset_{source} \quad (14)$$

where I is room thermal inertia and the ϕ_i are the amounts of heat transferred by the conduction from adjacent walls or from the outside or from possible sensible heat sources.

The humidity condition in the room is due to moisture transfer from interior surfaces, moisture production rate and the gains or losses due to air infiltration, natural and mechanical ventilation as well as sources or sinks due to the habitants of the room. This yields to the following mass balance equation for room air:

$$V\frac{\partial \rho_i}{\partial \tau} = Q_{mWest} - Q_{mEast} + Q_{mSouth} - Q_{mNorth} + Q_{mBottom} - Q_{mTop} + Q_{msource} \quad (15)$$

Radiation exchange in the room

In this work, the mean radiant temperature method is used to calculate long wave radiation exchange between walls. A linear equation expressing the radiative flow between a wall and all the other walls of the room is written as:

$$\emptyset_{rad,LW}^{int} = h_r S(T - T_m) \quad (16)$$

The value of h_r is expressed by:

$$h_r = 4\varepsilon\sigma_0 T_m^3 \quad (17)$$

Where T_m is the mean radiant temperature of the walls and is given by:

$$T_m = \frac{\sum S_j T_{Sj}}{\sum S_j} \quad (18)$$

For the shorts-wave radiation, we assumed that radiant energy enters the room by pane window and is distributed by the quota of 0.6 for the floor and 0.1 for the other walls.

Simulation Environment SPARK

To solve this system of equations, the Simulation Problem Analysis and Research Kernel (SPARK) is used. The latter allows solving efficiently differential equation systems (Sowell et al., 2001). Details of implementation and validation are shown in (Tran Le, 2009) and (Maalouf, 2014).

Results

In this study, two cases are presented and compared in terms of energy consumption. The first case considers only heat transfer within wall materials and the second case takes into account heat and moisture transfer within the building envelope. For both cases, simulations are run in a room of 23,1 m^2 and a volume of 65,8 m^3. The plan of the studied room is depicted in figure 5.

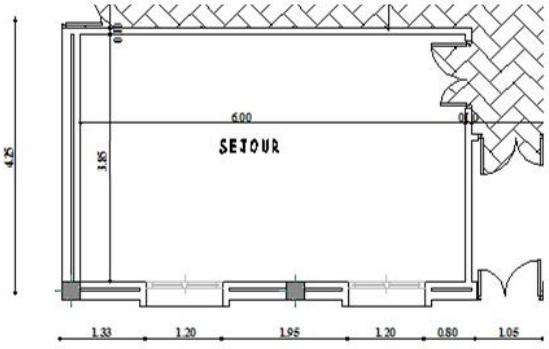

Figure 5: Plan of the studied room.

The Southern façade has two windows with simple glazing and an area of 1.2×1.4 m^2 each. The ceiling, the floor, the west and south facades are in contact with outdoor conditions while the other walls are considered as internal partitions. Details of wall composition are shown in table 5. The room is equipped with a heat sink and a PI controller that keeps the operating temperature between 19 °C and 26 °C during occupancy hours and between 18 and 26 °C by night. The room is occupied by two persons from 8 am to 19 pm. Air ventilation rate is taken to be 0.5 Vol/hr.

Wall	Wall composition and thickness
External vertical walls	Cement plaster (2cm), cork concrete L75 (15 cm), Cement plaster (2cm).
Internal partitions	Cement plaster (2cm), cork concrete L75 (10 cm), Cement plaster (2cm).
Roof	Cement plaster (2cm), cork concrete L75 (16 cm), reinforced concrete (7cm).
Floor	Carrelage (2cm), mortar (3cm), cork concrete L50 (12cm).

Table 5: Wall composition for studied room.

Convective heat transfer coefficients are $h_{T,e}$= 16 W/m^2.K for the outdoor surfaces and $h_{T,i}$= 3 W/m^2.K for indoor surfaces. Mass convection coefficients are respectively $h_{M,e}$= 0.005 m/s and $h_{M,i}$= 0.0025 m/s. The floor is considered impermeable to moisture. The initial relative humidity and temperature in the walls and the studied room were respectively equal to 50 % and 20 °C. Simulations are run for a period of 14 months, the results of the first two month are neglected and used to initialize simulation and results are presented for the last twelve months period from January to December. The weather data are those of Constantine in Algeria which has a Mediterranean weather, dry and hot in summer (temperature between 25 and 35°C, rarely exceeding 40°C) and mild and moist in winter (temperature between -2 and 12°C). The cement plaster layers are discretized in 5 nodes and the other layers are divided into 10 nodes. The time step is set to 360 s.

RESULTS

Heat transfer case

Table 6 compares room annual heating and cooling energy consumption when using wall composition of Table 4 for those using classical construction techniques.

	Heating energy consumption (kWh)	**Cooling energy consumption (kWh)**	**Annual energy consumption (kWh)**
With cork concrete L75-L50	2748	544	3292
Classical	3981	637	4618

Table 6: Annual heating and cooling energy consumption (kWh) for the studied room using cork concrete mixtures or classical construction case.

In the region which uses hollow brique (same composition of Table 4 in which cork concrete is replaced by same thickness hollow brick of thermal conductivity 0.5 W $m^{-1}K^{-1}$ and mass density 1900 kg m^{-3},for the roof hourdi blocks are used instead). It can be seen that the use of cork concrete reduces total energy consumption about 29%, this is due to the low thermal conductivity of the cork concrete aggregates which is lower than that of the hollow brick and hourdi. Other construction techniques are actually compared.

Heat and moisture transfer model

In this case we only consider the cork concrete wall case.

	Heating energy consumption (kWh)	**Cooling energy consumption (kWh)**	**Annual energy consumption (kWh)**
With cork L75-L50	2778	523	3301

Table 7: Annual heating and cooling energy consumption (kWh) for the studied room when taking into account heat and moisture transfer within building materials.

Table 7 shows heating and cooling energy consumption in the room when taking into account heat and moisture transfer within walls. Due to moisture desorption during the night, which is endothermic, heating energy consumption is slightly

higher and cooling consumption is lower as shown in Figure 6.

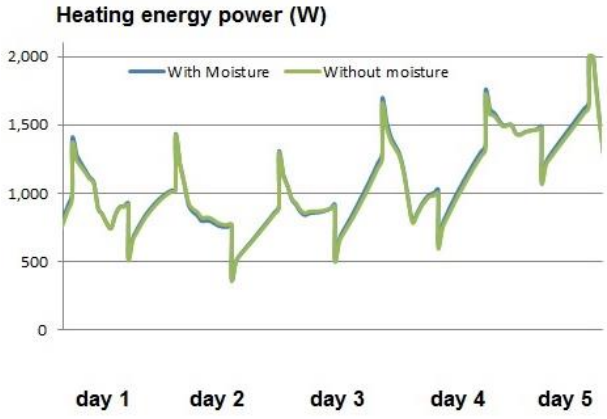

Figure 6 : Heating energy consumption during a week of December.

Figure 7 shows the indoor relative humidity pattern for both coupled heat and moisture transfer model and only heat transfer model. It can be seen that taking into account moisture transfer dampens relative humidity variation. This variation not only depends on cork concrete buffering value, but mainly on the cement plaster buffering value and hygric properties (its vapor resistance factor $\mu = 19$). The effect of plaster thickness will be studied.

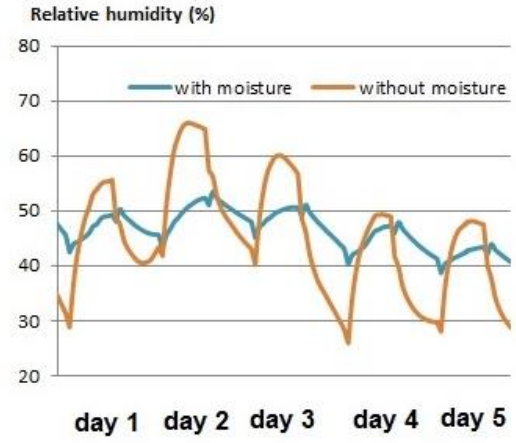

Figure 7 : Indoor relative humidity pattern during a week of December for both heat and moisture transfer case and only heat transfer case.

CONCLUSION

In this paper, two cork concrete mixtures are presented and their hygrothermal properties were measured. The MBV value was measured and it is found that the composition with 75% in volume of cork aggregates is a good humidity regulator. Hygrothermal properties are then used in the simulation environment SPARK to assess material hygrothermal performance on room level.
Simulations are run for a year for Constantine city weather conditions. Preliminary results show that cork concrete can reduce energy consumption about 29% when compared to a classical construction with hollow concrete. Taking into account moisture transfer increases slightly energy consumption in winter because of desorption phenomenon and reduces summer cooling energy. Further work will take into account hygrothermal building behaviour under different weather conditions, with natural ventilation model and other wall compositions.

NOMENCLATURE

Symbol	Definition	Unity
δ	Water vapour permeability	$Kg.m^{-1}.s^{-1}.Pa^{-1}$
δ_a	Air vapour permeability in the air	$Kg.m^{-1}.s^{-1}.Pa^{-1}$
ξ	Specific hygric capacity	-
∇P_v	Pressure gradient	Pa
μ	Material vapour resistance factor	
w	Moisture content by mass	Kg/Kg
C	Specific heat	$J.Kg^{-1}.K^{-1}$
C_0	Specific heat of dry material	$J.Kg^{-1}.K^{-1}$
C_l	Specific heat of water	$J.Kg^{-1}.K^{-1}$
D_T	Mass transport coefficient associated to a temperature gradient	$m^2.s^{-1}.K^{-1}$
$D_{T,v}$	Vapor transport coefficient associated to a temperature gradient	$m^2.s^{-1}.K^{-1}$
D_θ	Mass transport coefficient associated to a moisture content gradient	$m^2.s^{-1}$
$D_{\theta v}$	Vapor transport coefficient associated to a moisture content gradient	$m^2.s^{-1}$
g	Gravity acceleration	$m^2.s^{-1}$
h_M	Mass transfer convection coefficient	$Kg.m^{-2}.s^{-1}$
h_T	Heat transfer convection coefficient	$W.K^{-1}.m^{-2}$
L_v	Heat of vaporization	$J.Kg^{-1}$
R_v	Constant of water vapor	$J.Kg^{-1}.K^{-1}$
T	Temperature	K
Ta	Indoor air temperature	K
T_m	mean radiant temperature of the walls	K

T_0	operative temperature	K
t	Time	s
x	Abscise	m
θ	Moisture content	$m^3.m^{-3}$
λ	Thermal conductivity	$W.m^{-1}.K^{-1}$
ρ_0	Mass density of dry material	$Kg.m^{-3}$
ρ_l	Mass density of water	$Kg.m^{-3}$
ρ_v	Mass density of vapor water	$Kg.m^{-3}$
ψ	Capillary pressure	Pa
ψ_{tb}	Linear thermal bridge coefficient	$W.m^{-1}.K^{-1}$
ϕ	Relative humidity	%
ρ_i	Air density	$kg.m^{-3}$
Φ	Heat flux	W
Q_m	Air flow rate	$Kg.s^{-1}$
Φ_{source}	Heat source power	W
ε	Wall emissivity (long wave)	
σ_0	Stephan-Boltzmann constant	$W.m^{-2}.T^{-4}$

ACKNOWLEDGEMENT

The authors would like to thank “Lièges-Mélior” for providing cork aggregates.

REFERENCES

Aziz Ma., Murphy, Ck. and Ramaswamy Sd. 1979. Lightweight concrete using cork granules, International Journal of Lightweight Concrete, p. 29-33.

European Standards, EN 12667: 2001 Thermal performance of building materials and products (1 Ed.): Determination of thermal resistance by means clustering of guarded hot plate and heat flow meter methods. Products of high and medium thermal resistance.

Hagentoft C.E. 2001. Introduction to Building Physics. Studentlitteratur.

IUPAC. 1985. Reporting physisorption data for gas / solid systems with special reference to the determination of surface area and porosity area International Union of Pure and Applied Chemistry, p. 603-619.

Kunzel M. 1995. Simultaneous heat and moisture transport in building components, Fraunhofer Institute of building physics, Allemagne, 1995, disponible sur: http:// www.wufi.de/index_e.html (section: Literature).

Maalouf C., Tran Le A.D., Umurigirwa S.B, Lachi M., Douzane O. 2014. Study of hygrothermal behaviour of a hemp concrete building envelope under summer conditions in France. Energy and Buildings vol.77, p. 48-57.

Mendes N. 1997. Models for prediction of heat and moisture transfer through porous building element, Thèse de doctorat, 225, Federal University of Santa Catarina, Florianopolis, SC, Brésil.

Merakeb S., F. Dubois, Petit C. 2008. Modeling of the sorption hysteresis for wood. Wood Science Technology, vol. 43, p. 575-589.

Moreira A., Antonio J., Tadeu A. 2014. Lightweight screed Containing cork granules, Mechanical and Cement & Concrete hygrothermal characterization Composites, p.1-8.

NF EN ISO standard 12571: 2001 «Hygrothermal performance of building materials and products. Determination of water vapour transmission properties» AFNOR.

NF EN ISO standard 12572: 2000. Hygrothermal performance of building materials and products. Determination of hygroscopic sorption properties.

Philip, J.R., De Vries, D.A. 1957. Moisture movement in porous materials under temperature gradients, Transaction of American Geophysical Union. Vol .38, n.2, p.222-232.

Pedersen C.R. 1992. Prediction of moisture transfer in building constructions, Building and Environment, vol. 3, p.387–397.

Rode C. 2005. Moisture buffering of building materials. Report BYG DTU R-126; ISSN 1601–2917, ISBN 87-7877-195.

Sowell E.F., Haves P. 2001. Efficient solution strategies for building energy system simulation, Energy and Buildings, vol. 33, p. 309-317.

Tran Le A.D., Maalouf C., Mendoça K.C., Mai T.H., Wurtz E., 2009. Study of Moisture Transfer in a Double-Layered Wall with Imperfect Thermal and Hydraulic Contact Resistances, Journal of Building Performance Simulation, vol 2, p. 251-266.